

e.2



Lawrence Berkeley Laboratory

UNIVERSITY OF CALIFORNIA

RECEIVED
LAWRENCE
BERKELEY LABORATORY

Physics Division

JUN 18 1986

LIBRARY AND
DOCUMENTS SECTION

Presented at the XXIst Rencontre de Moriond on
Strong Interactions and Gauge Theories,
Les Arcs, France, March 16-22, 1986

DO THE CROSS SECTIONS FOR pp AND $p\bar{p}$
CONTINUE TO RISE AS $\log^2(s/s_0)$?

M.M. Block and R.N. Cahn

March 1986

TWO-WEEK LOAN COPY

*This is a Library Circulating Copy
which may be borrowed for two weeks.*



LBL-21402
e.2

DISCLAIMER

This document was prepared as an account of work sponsored by the United States Government. While this document is believed to contain correct information, neither the United States Government nor any agency thereof, nor the Regents of the University of California, nor any of their employees, makes any warranty, express or implied, or assumes any legal responsibility for the accuracy, completeness, or usefulness of any information, apparatus, product, or process disclosed, or represents that its use would not infringe privately owned rights. Reference herein to any specific commercial product, process, or service by its trade name, trademark, manufacturer, or otherwise, does not necessarily constitute or imply its endorsement, recommendation, or favoring by the United States Government or any agency thereof, or the Regents of the University of California. The views and opinions of authors expressed herein do not necessarily state or reflect those of the United States Government or any agency thereof or the Regents of the University of California.

March 1986

LBL-21402

**Do the Cross Sections for pp and $p\bar{p}$ Continue to Rise
as $\log^2(s/s_0)$?**

Martin M. Block

*Physics Department
Northwestern University
Evanston, IL 60201, USA*

and

Robert N. Cahn

*Lawrence Berkeley Laboratory
University of California
Berkeley, CA 94720, USA*

Presented by

Martin M. Block

at the XXIst Rencontre de Moriond on
Strong Interactions and Gauge Theories

March 16-22, 1986

Les Arcs, France

*This research was supported in part by the Director, Office of Energy Research,
Office of High Energy and Nuclear Physics, Division of High Energy Physics
of the U.S. Department of Energy under contracts*

DE-AC03-76SF00098 and DE-AC02-76-ER-02289 Task B.

I. INTRODUCTION

The advent of $p\bar{p}$ collider physics at the CERN ISR and Sp \bar{p} S during the last five years has extended the maximum $p\bar{p}$ center of mass energy from $\sqrt{s} \approx 20$ GeV to $\sqrt{s} = 900$ GeV. At the Sp \bar{p} S, experimental groups have measured σ_{tot} , the total cross section, and B, the nuclear slope parameter, at $\sqrt{s} = 540$ GeV, as well as σ_{tot} at $\sqrt{s} = 900$ GeV. In the energy range $30 \text{ GeV} < \sqrt{s} < 62 \text{ GeV}$, groups at the ISR have made precision measurements of these quantities for both $p\bar{p}$ and pp , with the same apparatus used to compare the $p\bar{p}$ and the pp system. Moreover, new ISR measurements of elastic scattering in the Coulomb interference region have made possible accurate determinations of ρ , the ratio of the real to the imaginary portion of the forward nuclear scattering amplitude, for both $p\bar{p}$ and pp . These new data, taken together with earlier results, now enables us to make a critical comparison of the $p\bar{p}$ and pp elastic scattering parameters in the high energy domain from $\sqrt{s} = 5$ GeV to $\sqrt{s} = 900$ GeV, and allow theoretical extrapolation to much higher energies. We will deal exclusively with $p\bar{p}$ and pp collisions, and in particular, will concern ourselves with the analysis of elastic scattering in the low $|t|$ region, $-t < 0.02 \text{ (GeV/c)}^2$, where t is the four-momentum transfer squared. The treatment follows a recent Review of Modern Physics article by M.M. Block and R.N. Cahn.^[1]

A model-free analysis will be made of the experimental quantities σ_{tot} , ρ and B. Traditionally, the requirements of analyticity have been compared with experimental data by means of dispersion relations. We will demonstrate how the same ends can be achieved more easily and transparently through direct use of simple analytic functions.

II. ANALYSIS OF $t=0$ AMPLITUDES

We define F as the analytic continuation of the forward scattering amplitude into the complex E plane, where E is the complex energy (E is the pp laboratory energy if E is real and $\geq m$, the nucleon mass). The F 's are real analytic functions having cuts on the real axis from $+m$ to ∞ and from $-m$ to $-\infty$. We choose the normalizations such, for fits with no odderons (unconventional odd amplitudes), the even continuation is,

$$4\pi F_+ = -\sqrt{(m+E)(m-E)} \left\{ A + \beta \frac{[\log(2m(m+E)/so) + \log(2m(m-E)/so)]/2i}{1 + a[\log(2m(m+E)/so) + \log(2m(m-E)/so)]/2i} + \frac{C}{2\sin(\pi\mu/2)} [2m(m+E)]^{\mu-1} + [2m(m-E)]^{\mu-1} \right\}, \quad (2.1a)$$

and the odd continuation is

$$4\pi F_- = -\sqrt{(m+E)(m-E)} \times \frac{D}{2\cos(\pi\alpha/2)} [2m(m+E)]^{\alpha-1} - [2m(m-E)]^{\alpha-1}, \quad (2.1b)$$

where A , β , so , a , C , μ , D , and α are real constants to be fitted by the data. Clearly, $F_+(E) = F_+(-E)$ and $F_-(E) = -F_-(-E)$. To find the scattering amplitudes for pp scattering, f_+ and f_- , we evaluate $F_+(E+i\epsilon)$ and $F_-(E+i\epsilon)$, in the limit of real E and $\epsilon \rightarrow 0$ (for the $p\bar{p}$ amplitudes, we evaluate the F 's at $-E-i\epsilon$). We obtain

$$\left(\frac{4\pi}{p}\right) f_+ = i \left\{ A + \beta \frac{[\log(2mp/so) - i\pi/2]i}{1 + a[\log(2mp/so) - i\pi/2]i} + C \left[\frac{((2m)(E-m))^{\mu-1} e^{i\pi(1-\mu)/2}}{2\sin(\pi\mu/2)} - \frac{((2m)(E+m))^{\mu-1} - ((2m)(E-m))^{\mu-1}}{2\sin(\pi\mu/2)} \right] \right\} \quad (2.2a)$$

and

$$\left(\frac{4\pi}{p}\right) f_- = D \left\{ \frac{((2m)(E-m))^{\alpha-1} e^{i\pi(1-\alpha)/2}}{2\cos(\pi\alpha/2)} + i \frac{((2m)(E+m))^{\alpha-1} - ((2m)(E-m))^{\alpha-1}}{2\cos(\pi\alpha/2)} \right\}. \quad (2.2b)$$

The optical theorem relates the cross sections σ^+ and σ^- to the above by

$$\sigma^\pm = \left(\frac{4\pi}{p}\right) \text{Im} f_\pm, \quad (2.3)$$

where p is the laboratory momentum. Hence, the imaginary portions of (2.2a) and (2.2b) give the appropriate cross sections, from which we form

$$\sigma(p\bar{p}) = \sigma^+ + \sigma^- \quad (2.4a)$$

and

$$\sigma(pp) = \sigma^+ - \sigma^- \quad (2.4b)$$

The formulae (2.2a) and (2.2b) simplify greatly in the limit of $E \gg m$,

where s is given by $s \sim 2mE \sim 2mp$. Using the notation $\langle f \rangle$ for the limit of f as $E \rightarrow \infty$, we find

$$\left(\frac{4\pi}{p}\right) \langle f \rangle_+ = i \left\{ A + \beta \frac{[\log(s/s_0) - i\pi/2]^2}{1 + a[\log(s/s_0) - i\pi/2]^2} + Cs^{\mu-1} e^{i\pi(1-\mu)/2} \right\} \quad (2.5a)$$

and

$$\left(\frac{4\pi}{p}\right) \langle f \rangle_- = -D \left\{ s^{\alpha-1} e^{i\pi(1-\alpha)/2} \right\}. \quad (2.5b)$$

If we put $a=0$ in (2.5a), we find by inspection of the real and imaginary parts of (2.5a) and (2.5b), the very useful and simple formulae,

$$\sigma(pp) = A + \beta \left[\log^2(s/s_0) - \frac{\pi^2}{4} \right] + C \sin\left(\frac{\pi\mu}{2}\right) s^{\mu-1} + D \cos\left(\frac{\pi\alpha}{2}\right) s^{\alpha-1}, \quad (2.6a)$$

$$\sigma(p\bar{p}) = A + \beta \left[\log^2(s/s_0) - \frac{\pi^2}{4} \right] + C \sin\left(\frac{\pi\mu}{2}\right) s^{\mu-1} - D \cos\left(\frac{\pi\alpha}{2}\right) s^{\alpha-1}, \quad (2.6b)$$

$$\rho(pp) = \left[\beta \pi \log(s/s_0) - C \cos(\pi\mu/2) s^{\mu-1} + D \sin(\pi\alpha/2) s^{\alpha-1} \right] / \sigma(pp), \quad (2.6c)$$

$$\rho(p\bar{p}) = \left[\beta \pi \log(s/s_0) - C \cos(\pi\mu/2) s^{\mu-1} - D \sin(\pi\alpha/2) s^{\alpha-1} \right] / \sigma(p\bar{p}). \quad (2.6d)$$

We have essentially used the forms (2.6a-d) in our earlier work^[2], where we introduced only the coefficients A , β , s_0 , D , α and a . We

interpret the even amplitude $Cs^{\mu-1}$ as an even Regge exchange term, and the odd amplitude $Ds^{\alpha-1}$ as an odd Regge exchange term. The term in β gives the $\log^2(s/s_0)$ rising cross section, and A corresponds to a constant cross section. It will turn out that the coefficients using (2.5a-b), i.e., using (2.6a-d), are nearly identical to those using the kinematically correct equations (2.2a-b). The only important difference is that (2.2a-b) give an improved χ^2 for the fit. This is because the low energy kinematics (the cut structure in E) is treated correctly in (2.2a-b) for $\sqrt{s} \sim 5$ GeV, where they are of importance. For $\sqrt{s} > 10$ GeV, the results using either (2.2a-b) or (2.5a-b) are numerically indistinguishable. The units are chosen such that σ is in mb, if E , m , p and \sqrt{s} are in GeV.

The introduction of an even Regge trajectory is a departure from our earlier treatment^[2]. We note that the $\log^2(s/s_0)$ term in the even amplitude, for $s < s_0$, simulates this term in the cross section. We have fixed the power μ to be 0.5, since we expect it to be about the same as α , which turns out to be ~ 0.5 .

Clearly, setting $a=0$ in (2.2a) gives rise to a cross section which continues to rise indefinitely as $\log^2(s/s_0)$. The introduction of a small, positive value of a in (2.2a) gives us a functional form which will have the cross section rise locally as $\log^2(s/s_0)$ (in the energy region $5 \text{ GeV} < \sqrt{s} < 62 \text{ GeV}$), However, as $s \rightarrow \infty$, i.e., at very high energies, the cross section will flatten out and go to the constant cross section, $A + (\beta/a)$, for positive a . Thus, we model the case where the Froissart bound is not truly saturated (it rises as $\log^2 s$ only

locally), and eventually the cross section rise stops, going to a constant cross section at ∞ . We consider this extreme case a measure of the deviation of the asymptotic behavior of the cross section from that of $\log^2(s/s_0)$.

Our original fits^[2], made several years ago for σ_{tot} and ρ for both the pp and $p\bar{p}$ systems, were for the energy domain $5 \text{ GeV} < \sqrt{s} < 62 \text{ GeV}$, and used about 80 pieces of data, including seven different types of experimental quantities, $\sigma(\text{pp})$, $\sigma(\text{p}\bar{\text{p}})$, $\rho(\text{pp})$, $\rho(\text{p}\bar{\text{p}})$, $\Delta\sigma = \sigma(\text{p}\bar{\text{p}}) - \sigma(\text{pp})$, $\Delta\rho = \rho(\text{p}\bar{\text{p}}) - \rho(\text{pp})$, and $\rho_{\text{av}} = [\rho(\text{p}\bar{\text{p}}) + \rho(\text{pp})]/2$. The χ^2 was minimized using the seven quantities and their quoted errors. No attempt was made to adjust any of the data systematically. The sources of the data are given in ref. [1]. The original fits were made before the earliest measurements of σ_{tot} at the SPS Collider. Those data were not included in our later work^[1] because they had large uncertainties and would not have had any statistical significance in our fits. These earlier studies showed:

1. The data were well fitted by simple functional forms using the proper analyticity. See Eqs (2.2a,b) or (2.5a,b).
- 2a. The data were consistent with a $\log^2(s/s_0)$ growth of σ_{tot} at high energy. $a=0$ in Eq (2.2a) or Eq (2.5a).
- 2b. The data were also consistent with a form for which σ_{tot} grew as

$\log^2(s/s_0)$ in the ISR energy region below $\sqrt{s} = 62 \text{ GeV}$, but asymptotically became constant. This form introduced the extra parameter a , but did not give a significantly better χ^2 . $a \neq 0$ in Eq (2.2a) or Eq (2.5a).

3. The data were consistent with the hypothesis that $\sigma_{\text{tot}}(\text{p}\bar{\text{p}}) - \sigma_{\text{tot}}(\text{pp}) \propto s^{-1/2}$. We were able to place impressive limits on "odderons", odd amplitudes corresponding to Regge trajectories with intercept $\alpha_{\text{odderon}} = 1$.
4. The conclusions were independent of the choice of \sqrt{s}_{min} from 5 to 15 GeV.

The purpose of this communication is to discuss the results of fits that include the recently published results of UA-1^[3], UA-4^[4], and UA-5^[5], as well as the lower energy data. The input for UA-5 was $\sigma_{\text{tot}} = 66.5 \pm 2.4 \text{ mb}$ at $\sqrt{s} = 900 \text{ GeV}$. For UA-1 and UA-5, the inputs for $\sqrt{s} = 540 \text{ GeV}$ were not the derived cross sections, but were the experimentally measured quantities: for UA-4, $\sigma_{\text{tot}}(1+\rho^2) = 63.3 \pm 1.5 \text{ mb}$, and for UA-1, $\sigma_{\text{tot}}(1+\rho^2)^{1/2} = 67.6 \pm 6.5 \text{ mb}$. Although the two measurements are consistent, the much smaller error for UA-4 makes it dominate in the fitting procedure at $\sqrt{s} = 540 \text{ GeV}$. The slope measurements at $\sqrt{s} = 540 \text{ GeV}$ were $15.2 \pm 0.2 \text{ GeV}^{-2}$ for UA-4 and $17.1 \pm 1.0 \text{ GeV}^{-2}$ for UA-1.

Listed in Table I are the features of fifteen different types of fits for σ_{tot} and ρ values, made both with and without the SpS points.

Since our previous studies showed that the odderon amplitudes were very small, we have not included them in this work. The even Regge trajectory ($C \neq 0$) with intercept $\mu=0.5$ was included in some fits, and excluded in others. Fits with asymptotic behavior $\sigma \propto \log^2(s/s_0)$ were tried ($a=0$), as well as ones with asymptotically constant behavior ($a \neq 0$). The functional form $\sigma \propto \log^\gamma(s/s_0)$ with $\gamma \neq 2$ was also investigated. Further, we investigated the sensitivity of our conclusions to our choice of \sqrt{s}_{\min} .

In Table II are shown the results of the fits that were made excluding the Sp \bar{p} S data, with γ set equal to 2 and $a=0$, so that $\sigma \propto \log^2(s/s_0)$ asymptotically. The fits are quite good and are insensitive to the inclusion of the lower energy data ($5 \text{ GeV} < \sqrt{s} < 15 \text{ GeV}$). The presence of the even Regge trajectory with $\mu = 0.5$ (fit #3, $C \neq 0$) has a rather minor effect on the other parameters, as well as on χ^2 .

Table III shows fits including the Sp \bar{p} S with γ still set equal to 2. It is clear that good fits are only obtained when $a \neq 0$, i.e., only when the cross section does not grow asymptotically as $\log^2(s/s_0)$. We conclude that the $\log^2(s/s_0)$ form is incapable of fitting both the Sp \bar{p} S data and the lower energy data simultaneously. This conclusion is unchanged either by restricting the data to $\sqrt{s} > 15 \text{ GeV}$ (fit #5) or including the even Regge term ($C \neq 0$, fit #7). The consequences of both restricting ourselves to only higher energy data and including the even Regge term ($C \neq 0$) are discussed in detail later. The values

of a obtained in the fits #6 and #8 are consistent with our pre-Sp \bar{p} S value, $a = 0.0056 \pm 0.0030^{[1,2]}$, but now have much greater statistical significance, being almost 6 standard deviations away from zero. Further, the functional forms which give asymptotically constant cross sections yield good χ^2 's. The value of a and its uncertainty are nearly completely determined by values of the high energy UA-4 and UA-5 points.

We illustrate fits #7 and #8 in Figs. 1a and 1b, where we plot σ_{tot} and ρ , respectively, as a function of \sqrt{s} . At lower energies, the pp and p \bar{p} data are clearly separated, with the pp data lower in value. In this region, fits #7 and #8 are indistinguishable. At higher energies, there is no distinction between pp and p \bar{p} , but fits #7 and #8 diverge. As seen in the figures, at high energies, fit #7 ($a=0$) gives higher values of σ_{tot} and ρ than does fit #8. For fits #4, #5 and #7, where σ_{tot} grows asymptotically as $\log^2(s/s_0)$, we obtain unsatisfactory χ^2 's. In particular, the UA-4 and UA-5 points are consistently lower than the fit and contribute inordinately to χ^2 . The UA-1 point, which is statistically much less significant, is not in disagreement with the fit, as seen in Fig. 1a.

The failure of the fits using $\log^2(s/s_0)$ with $a=0$ led us to investigate a more general class, where the exponent of the term in $\log(s/s_0)$ was varied from the Froissart bound value of 2, i.e., we let the cross section vary asymptotically as $\sigma \propto \log^\gamma(s/s_0)$, with γ as a free

parameter to be fitted from the data. The results are given in Table IV. The fits which include the Sp \bar{p} S points, #11 and #12, are unsatisfactory, again with UA-4 and UA-5 being the major contributors to the χ^2 . We note that all of the fits prefer a value of γ near the canonical value of 2. Thus, we clearly can not accommodate the Sp \bar{p} S points simply by changing the value of γ .

An early fit to the ISR data that has been widely used was presented in 1977 by Amaldi et al. [6] The form used was

$$\sigma_{\text{tot}} = B_1 + B_2(\log s)^\gamma + C_1 E^{-\nu_1} \pm C_2 E^{-\nu_2}, \quad (2.7)$$

where the upper sign is for pp and the lower is for p \bar{p} . It is important to note that in the second term of the Amaldi expression, s is measured in GeV², i.e., that s_0 , (the scale of s) is arbitrarily set to 1 GeV². Since the fit was made in 1977, there were no p \bar{p} data available in the ISR energy region to be used. Moreover, no values of $\rho(p\bar{p})$ were used in their fit at any energy. They calculated the values of $\rho(pp)$ by numerical means, using a singly subtracted dispersion relation, with the cross sections for pp and p \bar{p} parametrized by (2.7).

We have investigated fits of the type \log^γ , à la Amaldi, using our analytic technique, by setting $a=0$, $s_0=1$ GeV² and replacing the exponent 2 by the parameter γ in Eq (2.2a) or (2.5a), and by letting $C \neq 0$. Two fits were made, one in which μ was fixed at 0.5 and the

other with μ as a free parameter. The results are shown in Table V. We have included all of our usual data in the fit, including the Sp \bar{p} S points. The even Regge intercept μ is expected to be near 0.5, consistent with the value of the odd intercept α . If we fix μ to be 0.5, we get for fit #14 a χ^2 per degree of freedom, $\chi^2/\text{df} = 3.92$, which is obviously completely unsatisfactory. In fit #15, we allow μ to vary, and we obtain the best fit values $\mu = 0.78 \pm 0.03$ and $\gamma = 1.999 \pm 0.002$, with a $\chi^2/\text{df} = 1.24$. Although the χ^2/df is not unreasonable, the fit is highly suspect, since the value of μ is very far from the canonical value of 0.5, expected from a Regge analysis which justifies the inclusion of such an amplitude. We thus conclude that the Amaldi type of analysis cannot be reconciled with the full data set, even when varying γ .

The conclusions drawn from the fifteen fits described above are simple and quite straightforward. The fits that exclude the Sp \bar{p} S points are all satisfactory. The fits that include the Sp \bar{p} S points are satisfactory only if $a \neq 0$, i.e., unless the asymptotic growth of the total cross section is much slower than $\log^2(s/s_0)$. In particular, we get a satisfactory χ^2 if the cross section asymptotically approaches a constant. Since this is a most unexpected result, in our opinion, we have tried to investigate under what circumstances a $\log^2(s/s_0)$ growth of σ_{tot} is possible using the Sp \bar{p} S data points.

In fit #5, only data above $\sqrt{s} = 15$ GeV were used, with $C=0$. The fit was a failure. In fit #7, the full data set ($\sqrt{s} > 5$ GeV) was used,

but the even Regge trajectory ($C \neq 0$) with intercept $\mu = 0.5$ was included. This too was inadequate, yielding $\chi^2/df = 1.54$ (120/78). By combining the options of #5 and #7—restricting the data set to $\sqrt{s} > 15$ GeV and introducing the parameter $C \neq 0$ —we increase the chance of finding a reasonable fit. Such a fit—fit #16, which is described in Table VI—is subject however to serious objections. The even Regge term which is proportional to C describes a piece of the total cross section that vanishes as s goes to infinity. The restricted data set of fit #16 however covers almost exclusively the region of rising cross section, even for $p\bar{p}$. Without the many high precision datum points at the lower energies, the parameter C might well be taking on a new and anomalous role: it could now decouple the fit in the region $5 \text{ GeV} < \sqrt{s} < 62 \text{ GeV}$ from the fit to the $Sp\bar{p}S$ data.

Not surprisingly, this fit with $\sqrt{s} > 15$ GeV and $C \neq 0$ is successful, with $\chi^2/df = 1.14$ (35.2/31). Of course, we can not altogether dismiss this fit because of the inherent difficulties in fitting $C \neq 0$ at high energies. However, there are many features of fit #16 which set it apart from the other fifteen fits. All other 15 fits have β , the coefficient of the $\log^2(s/s_0)$ term, near the value 0.6, whereas here $\beta = 0.32$. Also, all other fits have s_0 near 300 GeV^2 , while for fit #16, $s_0 = 30 \text{ GeV}^2$. Further, those previous fits where $C \neq 0$ and so were fitted gave $C < 25$, whereas here $C = 69$.

This new fit differs dramatically from the others. If it is accepted,

then the others must be rejected. In its starkest form, we must choose between, say, fit #1, which utilizes 81 data points in the energy interval $5 \text{ GeV} < \sqrt{s} < 62 \text{ GeV}$, and fit #16, which uses 37 data points for $15 \text{ GeV} < \sqrt{s} < 900 \text{ GeV}$. We see that a good fit can be had either by dropping the UA-4 point at 540 GeV and the UA-5 point at 900 GeV, or, conversely, by ignoring the 47 data points below 15 GeV. We must make a subjective choice, since we have no a priori knowledge that our parametrizations of the amplitudes are adequate for the full energy region $5 \text{ GeV} < \sqrt{s} < 900 \text{ GeV}$. Nonetheless, one should be extremely cautious in embracing fit #16.

III. SLOPE ANALYSIS OF NEARLY-FORWARD ELASTIC SCATTERING DATA

The near-forward hadronic amplitude for $p\bar{p}$ and pp elastic scattering is reflected in three experimentally accessible parameters, the total cross section σ_{tot} , the ρ value, and the nuclear slope parameter $B(s)$, defined as

$$B(s) = \frac{d}{dt} \left[\log \left(\frac{dg}{dt} \right) \right]_{t=0} . \quad (3.1)$$

In Section II, we analyzed $t=0$ data for σ_{tot} and ρ , in order to extract the forward hadronic amplitudes f_+ and f_- . In this Section, we will use the results of Fit #2 to obtain the s dependence of the slopes B for pp and $p\bar{p}$ elastic scattering, using experimental data in the near-forward direction (defined as the small $|t|$ region, $-t < 0.02$

(GeV/c)²). We write the invariant hadronic differential scattering cross section as

$$\frac{d\sigma}{dt} = \frac{\pi}{p^2} |f_{+g_+}(t,s) \pm f_{-g_-}(t,s)|^2, \quad (3.2)$$

where p is the laboratory momentum. We have assumed real, exponential "form factors" in Eq. (3.2), with $g_{\pm}(t,s) = \exp(B^{\pm}t/2)$. Since we are only concerned with very small $|t|$, the assumption of an exponential is the practical equivalent of replacing $e^{Bt/2}$ with $1+Bt/2$. We rewrite Eq. (3.2) as

$$\frac{d\sigma}{dt} = \frac{\pi}{p^2} \left\{ [\text{Re}f_{+}\exp(B^{+}t/2) \pm \text{Re}f_{-}\exp(B^{-}t/2)]^2 + [\text{Im}f_{+}\exp(B^{+}t/2) \pm \text{Im}f_{-}\exp(B^{-}t/2)]^2 \right\}, \quad (3.3)$$

with the + sign for $p\bar{p}$ and the - sign for pp .

In our analysis, we will include slope data in the energy region $5 \text{ GeV} < \sqrt{s} < 62 \text{ GeV}$, and only those data measured in the low $|t|$ region, $-t \sim 0.02 \text{ (GeV/c)}^2$, in order to reasonably approximate the definition of B made in Eq. (3.1). The data do not form a smooth set, unlike the situation for σ_{tot} and ρ . In an earlier paper^[6], we discussed the choice of experimental data that have we employed. Since the total cross section is assumed to rise as $\log^2 s/s_0$, it is important to parameterize the B^{+} term, the even slope, with a corresponding $\log^2 s$ term.^[6] We choose

$$B^{+}(s) = C^{+} + D^{+}\log s + E^{+}\log^2 s \quad (3.4a)$$

and

$$B^{-}(s) = C^{-} + D^{-}\log s, \quad (3.4b)$$

where s is measured in $(\text{GeV})^2$. No attempt is made to adjust the data for systematic errors. The slope results with fits #3 and #7 used for $t=0$ amplitudes are given in Table VII.

Fig. 2 is a plot of our predicted values of B vs. \sqrt{s} , where the data used in the fit were in the energy interval $5 \text{ GeV} < \sqrt{s} < 540 \text{ GeV}$, and the results of fit #7 were used for the $t=0$ amplitudes.

IV. PREDICTIONS

Table VIII gives a summary of our high energy predictions for σ_{tot} and ρ , using fits #7 and #8. Table IX summarizes the predictions for the nuclear slope parameter B , using fit #7 for the $t=0$ amplitude.

V. CONCLUSIONS

It is most likely that the total cross section does not rise as $\log^2(s/s_0)$ if the UA-4 point at 540 GeV and the UA-5 point at 900 GeV

are correct. These experimental results are indeed compatible with the hypothesis that the total cross section asymptotically goes to a constant value. This completely unexpected and provocative result will have to be confirmed by measurements of either ρ at Sp \bar{p} S energies or σ and/or ρ at the Tevatron Collider ($\sqrt{s} = 2000$ GeV), an energy where measurements become definitive. It is clear that measurements of elastic pp and p \bar{p} scattering at ultra-high energies may still hold surprises for elementary particle physics.

VI. ACKNOWLEDGEMENTS

This research was supported in part by Department of Energy Contract DE-AC02-76-ER-02289 TaskB, at Northwestern University, and by Department of Energy Contract DE-AC03-76SF00098 at Lawrence Berkeley Laboratory, University of California. One of us (MMB) would like to thank the Aspen Center for Physics for its hospitality during the carrying out of this research and the writing of the manuscript.

References

- [1] M.M. Block and R.N. Cahn, Rev. Mod. Phys. 57, No. 2, 563 (1985).
- [2] M.M. Block and R.N. Cahn, Phys. Lett. 120B, 224 (1982).
- [3] UA-1 Collaboration, Phys. Lett. 128B, 336 (1983).
- [4] UA-4 Collaboration, Phys. Lett. 147B, 385 (1984); ibid. 392.
- [5] UA-5 Collaboration, Invited talk by P. Carlson, Div. of Particles and Fields, Am. Phys. Soc., Eugene, Oregon, August 12-15, 1985; private communication.
- [6] M.M. Block and R.N. Cahn, Phys. Lett. 120B, 229 (1982).

Figure Captions

1a. The total pp and $p\bar{p}$ cross section data and fits #7 and #8. At low energies, the pp data is lower than the $p\bar{p}$ data and the two fits coincide. At higher energies, the data coalesce but the predictions diverge. Fit #7 ($a=0$) lies higher than fit #8 ($a\neq 0$).

2a. The pp and $p\bar{p}$ ρ data and fits #7 and #8. At low energies, the pp data is lower than the $p\bar{p}$ data and the two fits coincide. At higher energies, the data coalesce but the predictions diverge. Fit #7 ($a=0$) lies higher than fit #8 ($a\neq 0$).

3. The slope data B and the fit. At lower energies, the pp slope is smaller than the $p\bar{p}$ slope. Fit #7 was used for the $t=0$ amplitude.

Table I

Characteristics of the fits to the cross sections and ρ data. When the even Regge trajectory is included ($C\neq 0$), μ is set equal to 0.5, except in fit #15.

Fit	Characteristics		
	Parameters	\sqrt{s}_{\min} (GeV)	Features
#1	5	5	No $Sp\bar{p}S$
#2	5	15	No $Sp\bar{p}S$
#3	6	5	No $Sp\bar{p}S$, $C\neq 0$
#4	5	5	$Sp\bar{p}S$
#5	5	15	$Sp\bar{p}S$
#6	6	5	$Sp\bar{p}S$, $a\neq 0$
#7	6	5	$Sp\bar{p}S$, $C\neq 0$
#8	7	5	$Sp\bar{p}S$, $C\neq 0$, $a\neq 0$
#9	6	5	No $Sp\bar{p}S$, $\gamma\neq 2$
#10	6	15	No $Sp\bar{p}S$, $\gamma\neq 2$
#11	6	5	$Sp\bar{p}S$, $\gamma\neq 2$
#12	7	5	$Sp\bar{p}S$, $\gamma\neq 2$, $C\neq 0$
#13	7	5	No $Sp\bar{p}S$, $\gamma\neq 2$, $C\neq 0$
#14	6	5	$Sp\bar{p}S$, $\gamma\neq 2$, $s_0=1 \text{ GeV}^2$, $C\neq 0$
#15	7	5	$Sp\bar{p}S$, $\gamma\neq 2$, $\mu\neq 0.5$, $s_0=1 \text{ GeV}^2$, $C\neq 0$

Table II

Fits to the data excluding Sp̄S points

Fit	#1	#2	#3
A	41.74 ± 0.37	41.66 ± 0.12	41.36 ± 0.25
β	0.66 ± 0.01	0.60 ± 0.04	0.63 ± 0.03
so	337 ± 8	306 ± 27	299 ± 25
D	-39.3 ± 1.6	-34.6 ± 6.8	-40.4 ± 1.8
α	0.48 ± 0.01	0.51 ± 0.04	0.47 ± 0.01
C	0	0	7.3 ± 4.6
χ ² /df	91.6/76=1.20	32.5/29=1.12	89.0/75=1.19

Table III

Fits to the data including Sp̄S points

Fit	#4	#5	#6	#7	#8
A	41.66 ± 0.04	41.34 ± 0.12	41.68 ± 0.04	40.42 ± 0.27	41.13 ± 0.22
β	0.62 ± 0.01	0.48 ± 0.03	0.63 ± 0.01	0.52 ± 0.02	0.59 ± 0.02
so	349 ± 8.4	242 ± 26	330 ± 7.6	217 ± 25	278 ± 21
D	-37.7 ± 1.5	-33.6 ± 6.2	-39.0 ± 1.5	-41.1 ± 1.9	-41.2 ± 1.9
α	0.49 ± 0.01	0.52 ± 0.04	0.48 ± 0.01	0.46 ± 0.02	0.46 ± 0.01
C	0	0	0	22.6 ± 4.5	10.5 ± 4.0
a	0	0	0.0083 ± 0.0013	0	0.0074 ± 0.0014
χ ² /df	146/79=1.85	51.9/32=1.62	86.1/78=1.10	120.4/78=1.54	78.9/77=1.02

Table IV

Fits with the variable γ in $\log^{\gamma}(s/s_0)$. Only fits #11 and #12 include the Sp \bar{p} S data.

Fit	#9	#10	#11	#12	#13
A	41.72 ± 0.04	41.70 ± 0.12	41.65 ± 0.04	40.33 ± 0.29	41.72 ± 0.40
β	0.66 ± 0.01	0.62 ± 0.04	0.61 ± 0.01	0.51 ± 0.02	0.66 ± 0.04
s_0	375 ± 20	335 ± 49	371 ± 21	195 ± 30	375 ± 72
D	-41.0 ± 1.9	-37.0 ± 8.4	-38.4 ± 1.7	-40.6 ± 1.9	-41.1 ± 1.9
α	0.46 ± 0.02	0.50 ± 0.05	0.48 ± 0.01	0.47 ± 0.02	0.46 ± 0.02
C	0	0	0	24.3 ± 4.6	0.1 ± 7.9
γ	2.015 ± 0.017	2.008 ± 0.011	2.009 ± 0.007	1.992 ± 0.007	2.015 ± 0.011
χ^2/df	86/75=1.15	32.0/28=1.14	145/78=1.86	118.8/77=1.54	86.4/74=1.17

Table V

Amaldi-type fits: $s_0 = 1 \text{ GeV}^2$. Fit #14 fixes $\mu = 0.5$ corresponding to $v_1=0.5$ in Eq (2.7), whereas fit #15 allows μ to vary.

Fit	#14	#15
A	32.57 ± 0.22	16.61 ± 3.26
β	0.16 ± 0.003	0.28 ± 0.02
s_0	1	1
D	-39.8 ± 2.0	-41.9 ± 2.1
α	0.47 ± 0.02	0.46 ± 0.02
C	80.9 ± 1.9	56.3 ± 1.7
γ	1.981 ± 0.003	1.999 ± 0.002
μ	0.5	0.779 ± 0.025
χ^2/df	305.4/78=3.92	95.3/77=1.24

Table VI

A fit to the data for $\sqrt{s} > 15$ GeV using the even Regge term ($C \neq 0$).

<u>Fit</u>	<u>#16</u>
A	36.37 ± 1.78
β	0.32 ± 0.046
so	30.1 ± 24.8
D	-41.0 ± 10.2
α	0.47 ± 0.05
C	69.2 ± 17.0
χ^2/df	$35.2/31=1.13$

Table VII

Fits for the slope parameters. See Eqs (3.4a), (3.4b).

<u>Fit</u>	<u>No SpES</u>	<u>With SpES</u>
C^+	10.79 ± 0.59	9.92 ± 0.31
D^+	-0.049 ± 0.202	0.27 ± 0.09
E^+	0.040 ± 0.017	0.013 ± 0.006
C^-	21.5 ± 5.1	18.9 ± 5.1
D^-	1.23 ± 1.08	1.93 ± 1.07
χ^2/df	$78.8/52=1.52$	$85.6/54=1.59$

Table VIII

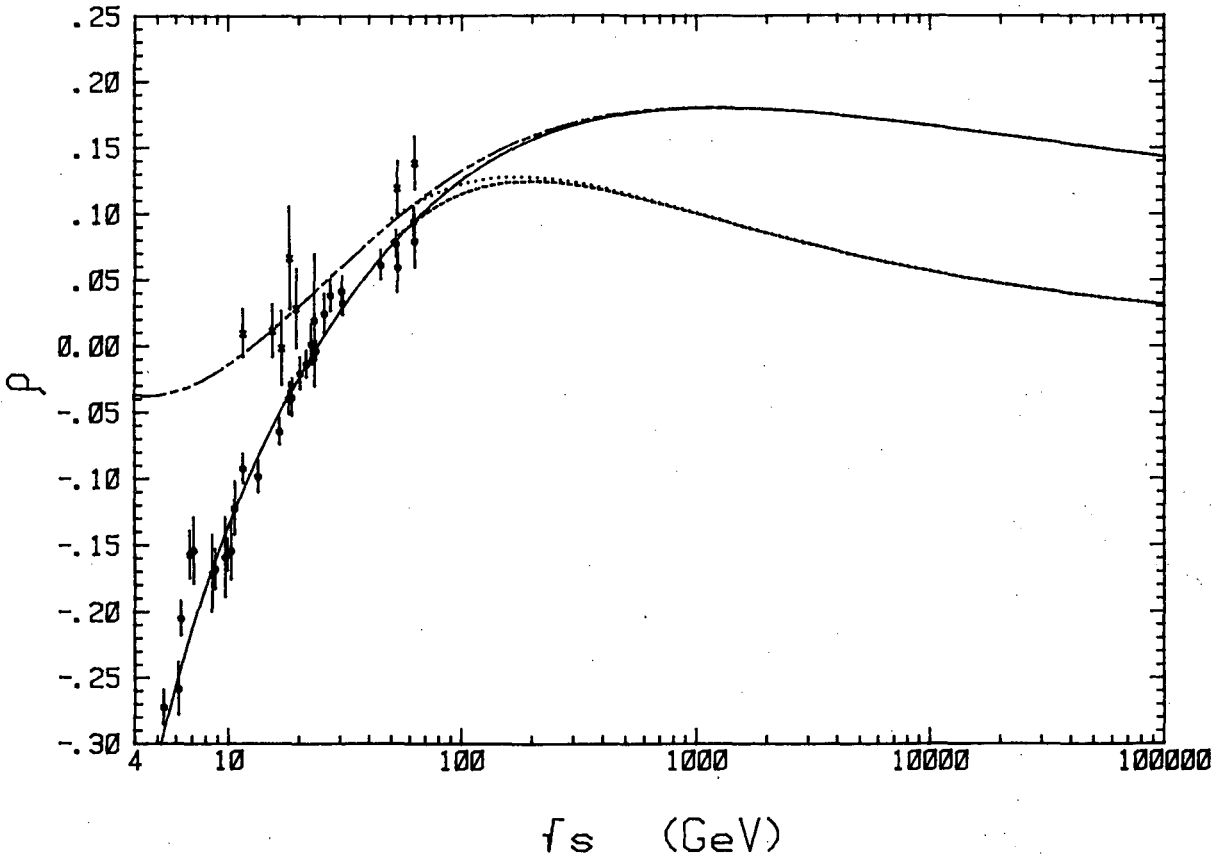
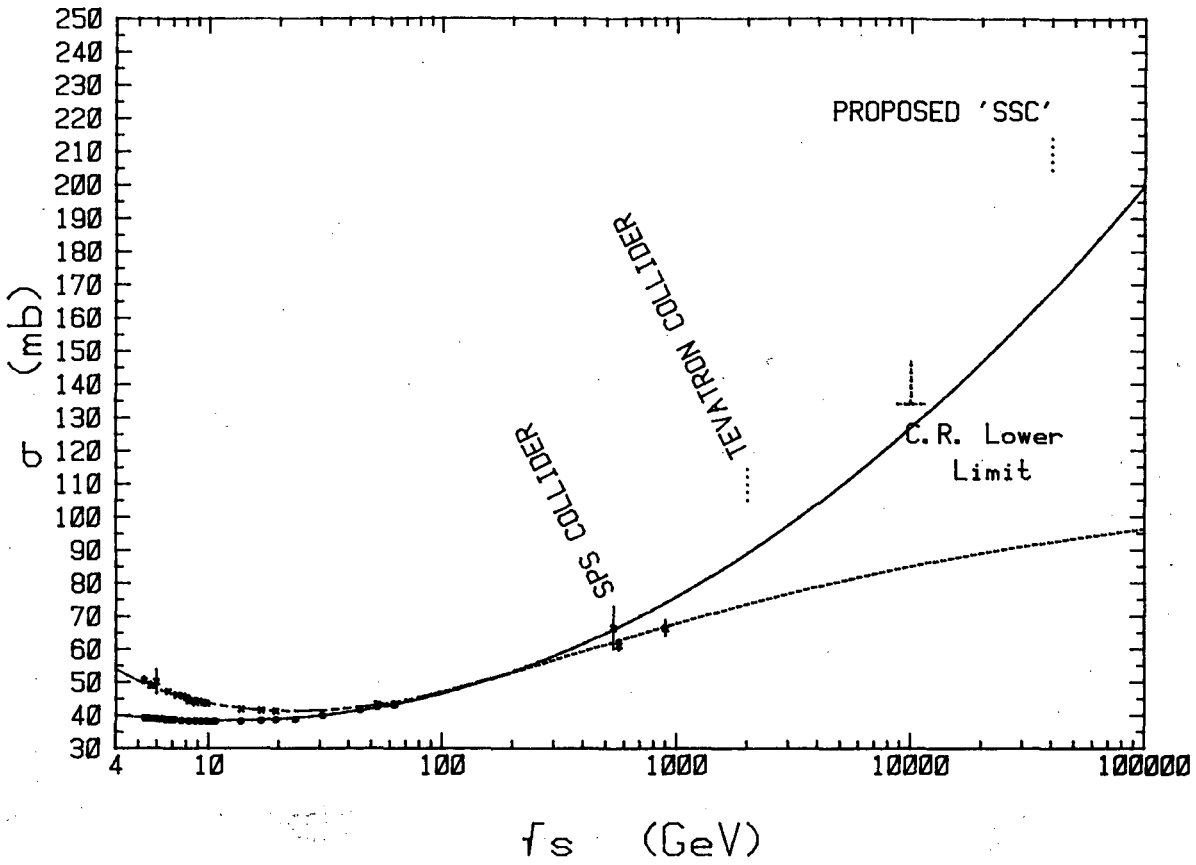
Predictions of fit #7 (a=0) and fit #8 (a≠0).

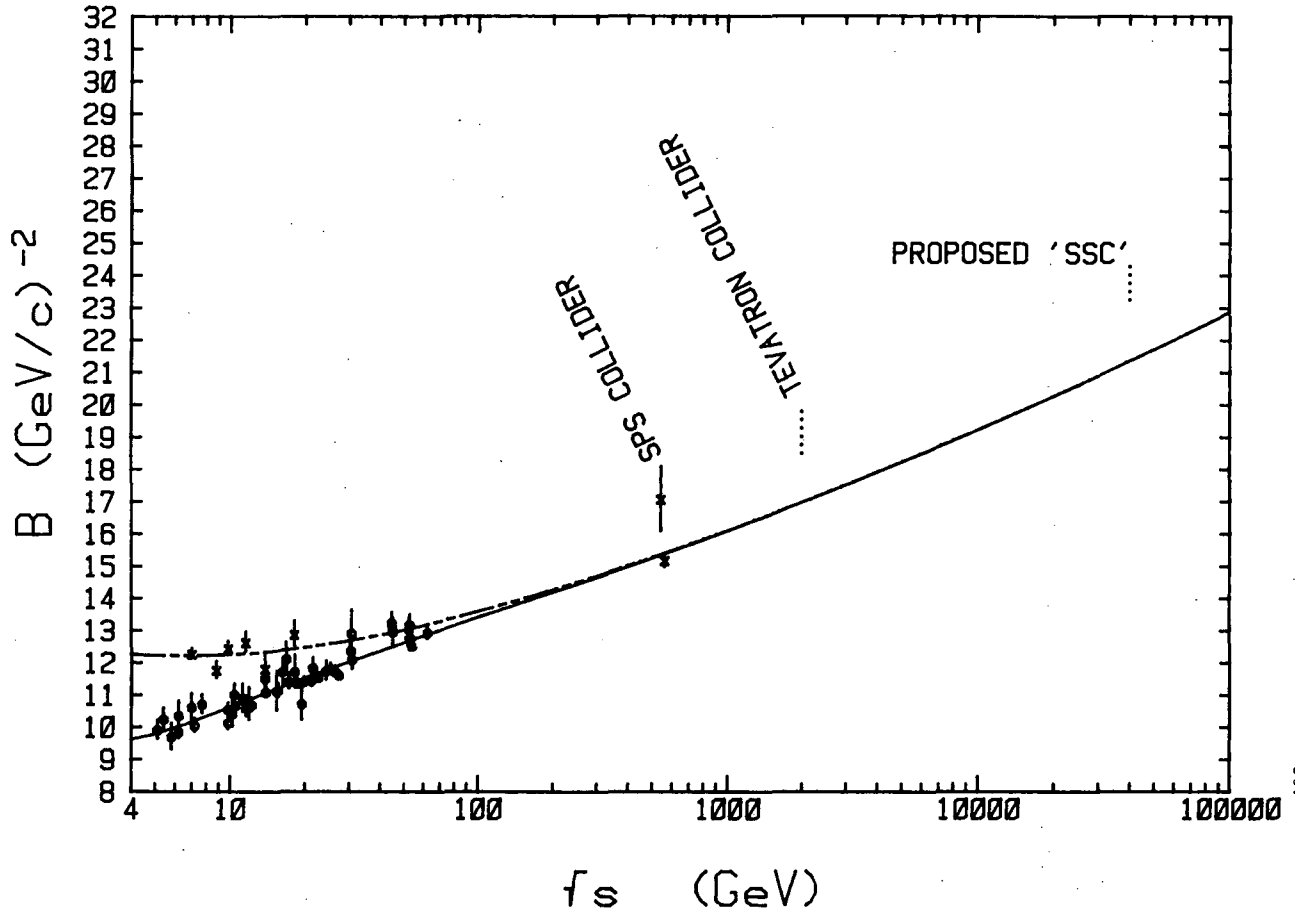
\sqrt{s} (TeV)	.540	.540	2.0	2.0	40.0	40.0
	$\sigma_{\text{tot}}(\text{mb})$	ρ	$\sigma_{\text{tot}}(\text{mb})$	ρ	$\sigma_{\text{tot}}(\text{mb})$	ρ
a=0	66.0±0.67	0.18±0.003	88.9±1.41	0.18±0.003	168.1±4.3	0.15±0.002
a=0.0074	62.2±0.94	0.11±0.009	73.7±2.26	0.09±0.010	92.5±5.7	0.04±0.007

Table IX

Predictions for the nuclear slope parameter B, using fit #7 for the t=0 amplitudes

\sqrt{s} (TeV)	B (GeV/c) ⁻²
.540	16.6 ± 0.5
2.0	19.4 ± 1.0
40.0	28.1 ± 2.6





This report was done with support from the Department of Energy. Any conclusions or opinions expressed in this report represent solely those of the author(s) and not necessarily those of The Regents of the University of California, the Lawrence Berkeley Laboratory or the Department of Energy.

Reference to a company or product name does not imply approval or recommendation of the product by the University of California or the U.S. Department of Energy to the exclusion of others that may be suitable.

*LAWRENCE BERKELEY LABORATORY
TECHNICAL INFORMATION DEPARTMENT
UNIVERSITY OF CALIFORNIA
BERKELEY, CALIFORNIA 94720*